Chaos, Solitons and Fractals 181 (2024) 114694

Contents lists available at ScienceDirect

Chaos, Solitons and Fractals

journal homepage: www.elsevier.com/locate/chaos

Entropy production on cooperative opinion dynamics

Igor V.G. Oliveira [a,b], Chao Wang [c,*], Gaogao Dong [d], Ruijin Du [e], Carlos E. Fiore [f], André L.M. Vilela [a,b,g,h], H. Eugene Stanley [h]

[a] Física de Materiais, Universidade de Pernambuco, Recife, PE 50720-001, Brazil
[b] Departamento de Física, Universidade Federal de Pernambuco, Recife, PE 50670-901, Brazil
[c] College of Economics and Management, Beijing University of Technology, Beijing, 100124, China
[d] School of Mathematical Sciences, Jiangsu University, Zhenjiang, 212013, China
[e] Center of Energy Development and Environmental Protection, Jiangsu University, Zhenjiang, 212013, China
[f] Instituto de Física, Universidade de São Paulo, São Paulo, SP, 05314-970, Brazil
[g] Data Science and Analytics, SUNY Polytechnic Institute, Utica, NY 13502, USA
[h] Center for Polymer Studies and Department of Physics, Boston University, Boston, MA 02215, USA

ARTICLE INFO

Keywords:
Complex systems
Consensus dynamics
Phase transition
Critical phenomena

ABSTRACT

As one of the most widespread social dynamics, cooperative behavior is among the most fascinating collective phenomena. Several animal species, from social insects to human beings, feature social groups altruistically working for a common benefit. This collaborative conduct pervades the actions and opinions of individuals, yielding strategic decision-making between political, religious, ethnic, and economic social puzzles. Here, we explore how cooperative behavior phenomena impact collective opinion dynamics and entropy generation in social groups. We select a random fraction f of community members as collaborative individuals and model the opinion dynamics using a social temperature parameter q that functions as a social anxiety noise. With probability q, regular individuals oppose their companions about a social decision, assuming group dissent. Collaborative agents experience a reduced effective social noise μq, where $0 < \mu < 1$ is the social anxiety noise sensibility parameter that enhances social validation. We perform numerical simulations and mean-field analysis and find the system undergoes nonequilibrium order–disorder phase transitions with expressive social entropy production. Our results highlight the effects of a social anxiety attenuation level in improving group consensus and the emergence of cooperative dynamics as a natural maximization of entropy production in noisy social groups, thus inducing exuberant collective phenomena in complex systems.

1. Introduction

In light of the pervasive influence of technology, the diverse and significant challenges surrounding information dissemination have propelled intense scientific research into Sociophysics models. Several dynamics regarding opinion formation on regular and complex networks were widely proposed to investigate social, financial, and professional interactions in groups of individuals or societies. Such physical models can capture the main features of complex collective phenomena in real societies. Similar to condensed matter systems, different opinion models exhibit intense critical dynamics and nontrivial nonequilibrium phase transitions [1–25].

Within the Sociophysics framework, the majority-vote model is an agent-based representation of interacting individuals in a contact network [24–45]. The model consists of a system of agents that hold opinions for or against some issue, and the stochastic variable σ_i, which assumes one of the two values ± 1, represents the opinion of an individual i at a given time. The majority-vote model evolves by an inflow dynamics, where each agent agrees with the majority of its neighbors with probability $1 - q$ and disagrees with chance q. The quantity q is called the noise parameter of the model, and it relates to a level of social anxiety, or social temperature, of the system.

Among several variations of this model, we highlight the investigation of majority-vote dynamics under the framework of random graphs and complex networks of interactions. In these studies, the authors find that group ordering, or opinion polarization in a society, is strongly related to the number of interacting neighbors [29–34], while additional investigations focus on social dynamics of systems composed of heterogeneous agents [35–38,41].

Inspired by real-world social group behavior, scientists developed further generalizations of the model, such as the three-state interpretation and different opinion functions, under the influence of regular and

* Corresponding author.
E-mail address: chaowanghn@vip.163.com (C. Wang).

https://doi.org/10.1016/j.chaos.2024.114694
Received 13 January 2024; Received in revised form 26 February 2024; Accepted 1 March 2024
Available online 11 March 2024

complex networks [43–48]. Nonetheless, based on opinion dynamics, examinations of this model rendered insights on second-order phase transitions, proposing criteria for the volumetric scaling of physical quantities at the critical point, yielding a universal relation for critical exponents regardless of the structure of the interaction network [48]. Recent studies on the economic behavior of brokers in financial markets reproduced real-world market features apprised by majority-vote dynamics [49–52].

Cooperative behavior is one of the most widespread collective social phenomena that still challenge scientists. Several animal species, from insects to human beings, exhibit social groups working for a joint benefit. Typical cooperative behavior, such as group hunting and reciprocity protection, makes species more competitive. Without this phenomenon, social institutions, non-governmental organizations, governments, culture, education, transport, health systems, among others, could be unattainable. Collaborative manners permeate the actions and opinions of individuals, imbuing strategic decision-making related to social dilemmas such as political, religious, ethnic, and economic challenges [53–55]. In this paper, we design an anisotropic social model to investigate the influence of cooperative voters on group opinion evolution.

We propose an agent-based model with two types of individuals, collaborative and regular, who exhibit different chances to adopt the dominant opinion expressed in a social group. We introduce a parameter $\mu \in (0,1)$, named noise sensibility, to the standard majority-vote model to yield a distinct influence of social anxiety over individuals. Hence, a cooperative individual is under an effective attenuated social temperature μq, while a regular individual is subject to the regular noise q.

Our results show that the consensus is strongly related to the number of collaborative individuals and noise sensibility. Numerical and analytical results add a significant new twist to the remarkable observation of the entropy flux of the mean-field majority-vote model [56–58]. We achieve a general expression for isotropic and anisotropic cases and verify our results using numerical simulations in the mean-field formulation.

2. Model

In the isotropic majority-vote model (MVM), each agent occupies a node i of a given network of social interactions. A spin variable σ_i represents the opinion of the agent i about a particular subject or in a referendum in an instant t. In the isotropic version, an individual is under a probability $1-q$ that its opinion σ_i follows the majority state of its interacting neighbors while assuming the minority state with probability q [24,25].

In this work, we analyze a square lattice opinion network with L^2 nodes, where a randomly chosen fraction f of agents have noise sensibility $0 < \mu < 1$, addressing the behavior of the cooperative individuals. In contrast, the complementary fraction $1-f$ of regular voters follow the standard majority-vote dynamics, i.e., $\mu = 1$. Thus, for noise level q, we denote the flipping probability of a given opinion σ_i as

$$w_i(\sigma) = \frac{1}{2}\left[1 - (1-2\mu_i q)\sigma_i S\left(\sum_{\delta=1}^{4}\sigma_{i+\delta}\right)\right], \tag{1}$$

the summation runs over all the four first neighboring opinions that influence the individual i and $S(x)$ stands for the signal function, where $S(x) = -1, 0, 1$ for $x < 0$, $x = 0$, and $x > 0$, respectively. Furthermore,

$$\mu_i = \begin{cases} \mu, & \text{if } i \text{ is a cooperative agent.} \\ 1, & \text{if } i \text{ is a regular agent.} \end{cases} \tag{2}$$

That is, a cooperative individual agrees with the majority with probability $1-\mu q$, and disagrees with probability μq. Thus, noise sensibility $\mu < 1$ increases the agreement probability by attenuating the effect of the noise parameter q on society.

The cooperative majority-vote dynamics with $f = 0$ capture the behavior of the isotropic majority-vote model with noise [24,25]. For $f = 1$, all individuals are cooperative, and the system also behaves as the standard MVM under the linear transformation $q \longrightarrow q/\mu$. In contrast, highlighting the effects of the noise sensibility μ, we recover the standard flip probability of the isotropic MVM when $\mu = 1$, in which all the agents are under the influence of the same social temperature q. The case for $\mu = 0$ corresponds to a bimodal distribution of noise, where a fraction f of the individuals are noiseless, always agreeing with its nearest interacting neighbors, scrutinized in previous investigations [36,41]. In this research, we perform numerical Monte Carlo simulations and a mean-field analytical procedure for the general cases of $0 < f < 1$ and $0 < \mu < 1$.

3. Cooperative stationary dynamics

To investigate the critical behavior of the model, we consider the order parameter m given by

$$m = \frac{1}{L^2}\left|\sum_{i=1}^{L^2}\sigma_i\right|. \tag{3}$$

We also consider magnetization $M_L(q,\mu,f)$, magnetic susceptibility $\chi_L(q,\mu,f)$, and Binder fourth-order cumulant $U_L(q,\mu,f)$

$$M_L(q,\mu,f) = \langle\langle m\rangle_t\rangle_c, \tag{4}$$

$$\chi_L(q,\mu,f) = L^2\left[\langle\langle m^2\rangle_t\rangle_c - \langle\langle m\rangle_t\rangle_c^2\right], \tag{5}$$

$$U_L(q,\mu,f) = 1 - \frac{\langle\langle m^4\rangle_t\rangle_c}{3\langle\langle m^2\rangle_t\rangle_c^2}, \tag{6}$$

where $\langle\ldots\rangle_t$ represents time averages taken in the stationary regime, and $\langle\ldots\rangle_c$ stands for configurational averages taken over independent realizations.

We perform Monte Carlo simulations on square lattice networks with L ranging from 40 to 200 and periodic boundary conditions. One Monte Carlo step (MCS) corresponds to the trial of updating N opinions randomly chosen accordingly to (1). Next, we discard 2×10^4 MCS to allow the system to reach the steady state and take the time averages over the subsequent 10^5 MCS. We repeat the process up to 100 independent samples to compute configurational averages. In our results, the statistical uncertainty is smaller than the symbol size.

In Fig. 1, we deliver snapshots of simulations for square lattices with $L = 200$, $q = 0.12$ and $\mu = 0.5$, for different values of collaborative fraction f: (a) 0.00, (b) 0.20, (c) 0.50 and (d) 1.00. White and black dots represent opinions +1 and −1, respectively. For fixed levels of μ and q, the collaborative agents increase the local consensus around them by supporting their contacts' opinions. This collective phenomenon yields a white cluster of agents with the same opinion, which increases with the fraction f of cooperative agents in figures (a) to (d), thus promoting social order.

Fig. 2 illustrates how the cooperative fraction of agents f improves social order when they have a 50% boosted chance of agreeing with their neighbors ($\mu = 0.5$). We plot (a) magnetization $M_L(q,\mu,f)$, (b) susceptibility $\chi_L(q,\mu,f)$, and (c) Binder cumulant $U_L(q,\mu,f)$ versus cooperative fraction f for $L = 200$, $\mu = 0.5$ and several values of q. Note that for each level of social anxiety q, the system undergoes a disorder–order transition for increasing values of f, agreeing with Fig. 1. We highlight the limiting cases $q = 0$ and $q = 0.3$ for $\mu = 0.5$ in Fig. 2(a), which are insensitive to f.

Fig. 3 shows how the nonconformity parameter q affects societies with different fractions of cooperative individuals for noise sensibility fixed at $\mu = 0.5$. We plot (a) magnetization $M_L(q,\mu,f)$, (b) susceptibility $\chi_L(q,\mu,f)$, and (c) Binder cumulant $U_L(q,\mu,f)$ versus social anxiety level q for $L = 200$. For small noise q, $M_L(q,\mu,f) = O(1)$ indicates the ordered phase of the social system with one dominant opinion. By

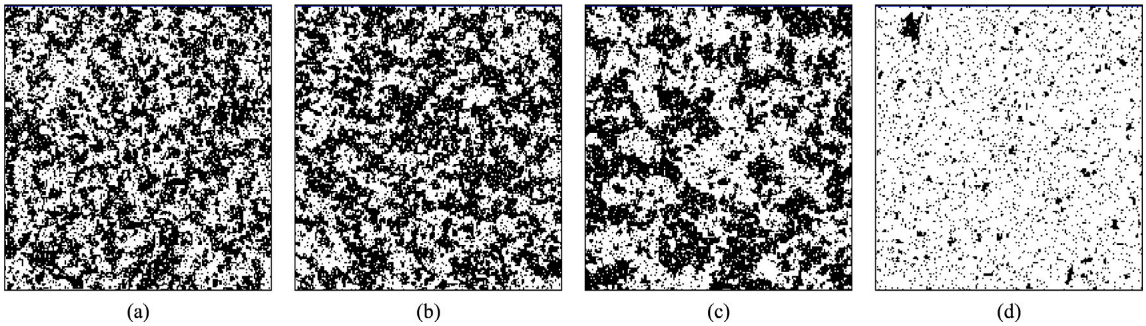

Fig. 1. Snapshots of a single simulation on a square network with $L = 200$, $q = 0.12$ and noise sensibility $\mu = 0.5$. (a) cooperative fraction $f = 0.00$, (b) $f = 0.20$, (c) $f = 0.50$, and (d) $f = 1.00$. Increasing f promotes social system consensus. White (black) dots represent +1 (−1) opinions.

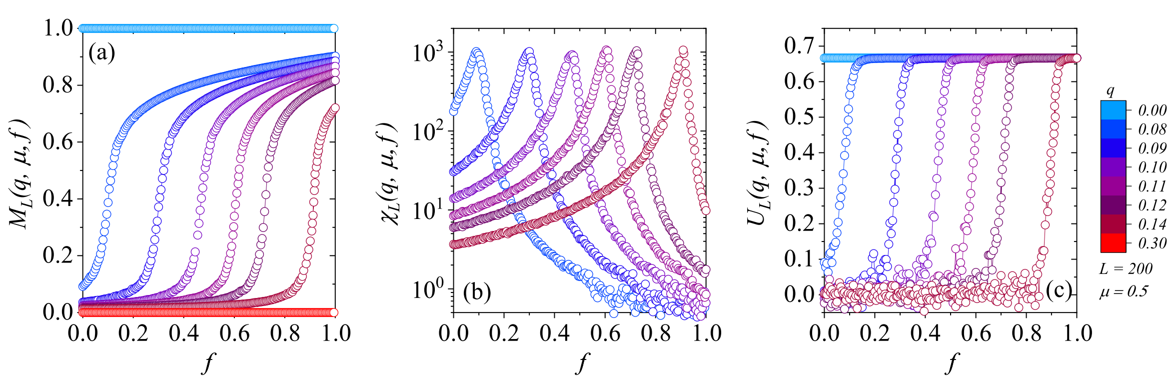

Fig. 2. Disorder–order transitions induced by the fraction of cooperative agents. In this configuration, $L = 200$ and $\mu = 0.5$ for different values of q. Figures (a), (b), and (c) stand for magnetization, susceptibility, and Binder cumulant, respectively. From left to right, $q = 0.08, 0.09, 0.10, 0.11, 0.12$ and 0.14. Results for $q = 0.0$ and $q = 0.3$ are insensitive to f for $\mu = 0.5$.

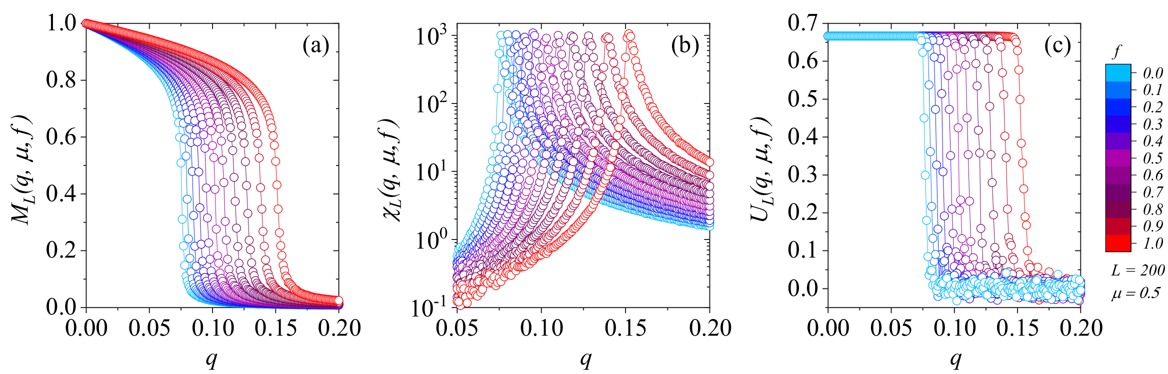

Fig. 3. Stationary averages of the cooperative majority-vote opinion dynamics. Square lattice simulations for $L = 200$, $\mu = 0.5$, and several values of f. Noise dependence of (a) average opinion (b) susceptibility, and (c) Binder cumulant. From left to right, f increases from 0.0 to 1.0 with $\Delta f = 0.1$ increments. The lines are guides to the eyes.

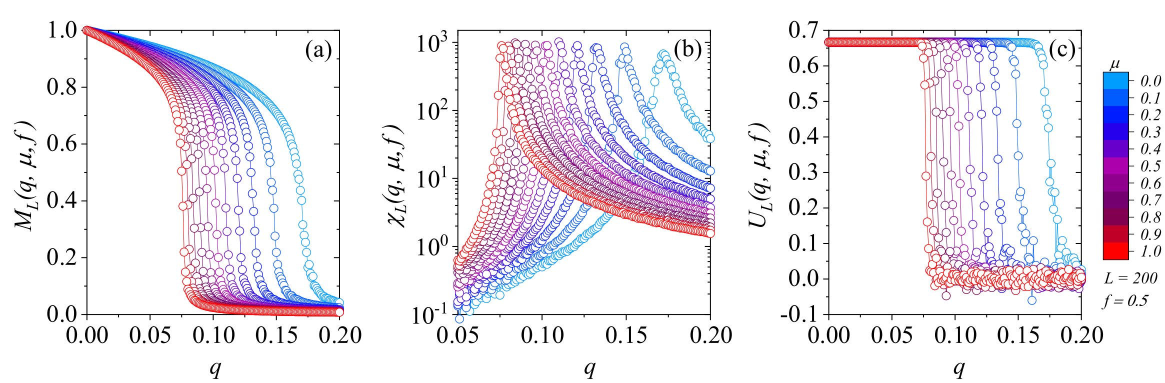

Fig. 4. Effects of the intensity μ of cooperative behavior on consensus robustness. (a) Magnetization $M(q, \mu, f)$, (b) magnetic susceptibility $\chi(q, \mu, f)$ and (c) Binder fourth-order cumulant $U(q, \mu, f)$ for diverse values of μ. From right to left, μ changes from 0.0 to 1.0 with $\Delta \mu = 0.1$ and $f = 0.5$. The lines are guides to the eyes.

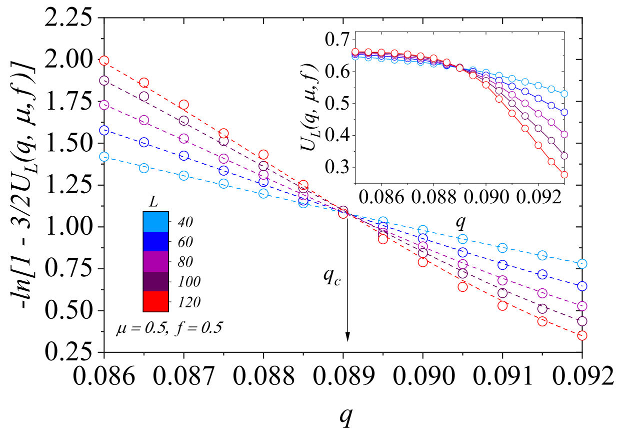

Fig. 5. Critical noise estimative. Binder fourth-order cumulant $U_L(q,\mu,f)$ for $\mu = 0.5$ and cooperative fraction $f = 0.3$. The point where the curves for different sizes L intersect provides an estimate for critical social temperature $q_c(\mu,f)$ in the thermodynamic limit $N \to \infty$. The dashed lines are cubic fits of the data points in critical region, and the continuous lines are guides to the eyes.

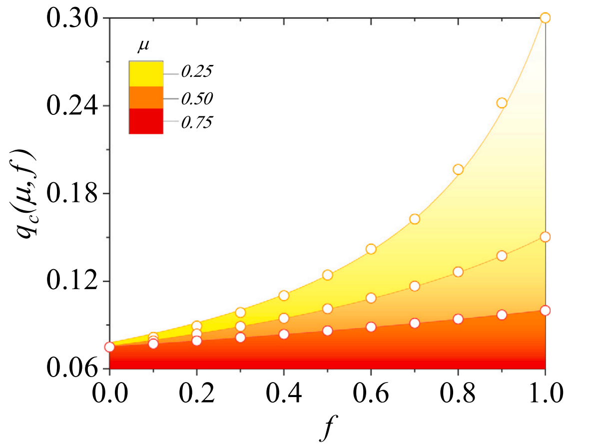

Fig. 6. Phase diagram of cooperative majority-vote opinion dynamics. The curves are descriptions of the phase boundary that separates the ordered and disordered phases for different values of noise sensibility μ. Circles represent the numerical estimates of critical points $q_c(\mu,f)$, obtained by the crossing point of the Binder cumulant curves for different system sizes. Lines are fits from Eq. (7).

increasing social temperature q, $M_L(q,\mu,f)$ decreases to zero for all values of the cooperative fraction f at a critical noise level $q = q_c(\mu,f)$. Systems with more cooperative agents support partial consensus for higher social temperatures, yielding a higher critical noise $q_c(\mu,f)$.

For $q > q_c(\mu,f)$, $M_L(q,\mu,f) \approx 0$, and the community exhibits two opinions approximately in the same share, not supporting consensus even with the presence of cooperative individuals. The system undergoes a second-order phase transition near a critical temperature $q_c(\mu,f)$, where the magnetic susceptibility $\chi_L(q,\mu,f)$ exhibits a maximum and the Binder cumulant $U_L(q,\mu,f)$ decreases swiftly. We remark that the critical noise value is an increasing function of the cooperative fraction f since such agents improve consensus.

In Fig. 4, we study how different intensities of the cooperative behavior phenomena influence consensus when half of the community is collaborative $f = 0.5$. We investigate the behavior of (a) magnetization $M_L(q,\mu,f)$, (b) susceptibility $\chi_L(q,\mu,f)$, and (c) Binder cumulant $U_L(q,\mu,f)$ as a function of q for $L = 200$ and diverse values of the noise sensibility μ. Decreasing μ stimulates the individuals to cooperate, reinforcing robustness to opinion disorder. Consequently, we observe that the critical noise $q_c(\mu,f)$ is a monotonically decreasing function of the noise sensibility μ for a non-zero fraction of cooperative agents.

Observe that as μ decreases, the range of social temperatures q for which the community exhibits a partial consensus increases. Indeed, each cooperative individual serves as a social influence on their neighbors, promoting the growth of a consenting cluster. This phenomenon directly affects the critical noise $q_c(\mu,f)$, in which $M(q_c) \to 0$. We conclude that the critical noise is a monotonically decreasing function of μ for a non-zero fraction of cooperative agents.

3.1. Phase diagram

To obtain a precise estimate of the critical social temperature $q_c(\mu,f)$ in the thermodynamic limit $N \to \infty$, which is independent of the society scale L, we calculate the Binder fourth-order cumulant for each pair (μ,f) with different system sizes. In Fig. 5, we exemplify this method by displaying the Binder cumulant for $\mu = 0.5$ and $f = 0.3$. We estimate the critical noise value $q_c(\mu,f)$ from the intersection point of Binder curves for different sizes L, since U does not depend on the system size only at $q = q_c(\mu,f)$. We find $q_c(\mu,f) = 0.0891(2)$ for $\mu = 0.5$ and $f = 0.3$. In Table 1, we summarize the results for the same process employing other values of f and μ, rendering the phase diagram shown in Fig. 6.

The interpolation of critical points $q_c(\mu,f)$ in Fig. 6 generates a description of the phase boundary that separates the ordered and disordered phases for each value of the noise sensibility μ. We note that consensus correlates with noise sensibility, and lower values of μ tend to yield higher values of q_c. Consensus robustness is also proportional to f since it controls the fraction under the influence of an effective noise reduction. From the data, we propose the phase boundary lines to obey an equation of type

$$q_c(\mu,f) = \frac{1}{a - bf}, \tag{7}$$

in which a and b are parameters that depend on μ. By conducting a non-linear curve fitting using Eq. (7), we estimate $[a,b] = [12.8(5), 9.4(5)], [13.2(1), 6.5(1)], [13.2(1), 3.3(1)]$, for $\mu = 0.25, 0.50$ and 0.75, respectively. From Table 1, we obtain $q_c(\mu,0) = 1/a \approx 0.075$, in agreement with the isotropic MVM [24], and $q_c(\mu,1) = 1/(a-b) \approx 0.075/\mu$ as expected from previous analysis.

3.2. Critical exponents

We examine finite-size effects on the social dynamics of the cooperative majority-vote model. In Fig. 7, we exhibit (a) magnetization, (b) susceptibility and (c) Binder cumulant for $f = 0.8$ and $\mu = 0.5$, with $L = 40, 60, 80, 100$ and 120. Note that at the critical point $q_c(\mu,f) \approx 0.13$ (see Table 1), $M \to 0$ as $L \to \infty$, remaining non-zero for noise values below $q_c(\mu,f)$. Also, the larger L, the more intense the magnetization fluctuations, yielding the highest peaks observed for the magnetic susceptibilities near $q_c(\mu,f)$.

To further analyze the behavior of M, χ, and U with system size L near the critical point, we estimate the critical exponents β/ν, γ/ν, and $1/\nu$ that characterize the phase transition of the model. Thus, we write the following finite-size scaling relations

$$M_L(q,\mu,f) = L^{-\frac{\beta}{\nu}} \widetilde{M}(\varepsilon L^{\frac{1}{\nu}}), \tag{8}$$

$$\chi_L(q,\mu,f) = L^{\frac{\gamma}{\nu}} \widetilde{\chi}(\varepsilon L^{\frac{1}{\nu}}), \tag{9}$$

$$U_L(q,\mu,f) = \widetilde{U}(\varepsilon L^{\frac{1}{\nu}}), \tag{10}$$

where $\varepsilon = q - q_c(\mu,f)$ is the distance from critical noise, and the universal scaling functions $\widetilde{M}$, $\widetilde{\chi}$ and $\widetilde{U}$ depend only on scaling variable $x = \varepsilon L^{\frac{1}{\nu}}$. Accordingly, we use these equations to obtain the phase transition critical exponents and capture the universal behavior of magnetization, magnetic susceptibility, and Binder cumulant.

In Fig. 8, we illustrate the numerical results for (a) M, (b) χ and (c) U versus the system size L at $q_c(\mu,f)$, with $\mu = 0.5$ and several values

Table 1
Critical social temperatures on square lattices and mean-field numerical estimates $q_c(\mu, f)$ and $q_c^{MF}(\mu, f)$, respectively, as a function of f and μ for the cooperative majority-vote dynamics.

f	$q_c(\mu = 1/4)$	$q_c(\mu = 1/2)$	$q_c(\mu = 3/4)$	$q_c^{MF}(\mu = 1/4)$	$q_c^{MF}(\mu = 1/2)$	$q_c^{MF}(\mu = 3/4)$
0.0	0.0750(1)	0.0750(3)	0.0750(1)	0.1665(1)	0.1665(1)	0.1664(3)
0.1	0.0816(2)	0.0791(2)	0.0771(1)	0.1802(1)	0.1753(1)	0.1711(2)
0.2	0.0894(1)	0.0839(1)	0.0792(1)	0.1957(3)	0.1851(1)	0.1750(1)
0.3	0.0986(1)	0.0891(2)	0.0814(1)	0.2149(1)	0.1961(1)	0.1799(2)
0.4	0.1101(2)	0.0947(2)	0.0837(1)	0.2376(4)	0.2077(3)	0.1848(1)
0.5	0.1243(1)	0.1011(1)	0.0861(2)	0.2667(1)	0.2224(2)	0.1904(1)
0.6	0.1420(3)	0.1085(2)	0.0886(2)	0.3031(3)	0.2373(1)	0.1955(1)
0.7	0.1626(3)	0.1167(2)	0.0912(2)	0.3507(1)	0.2566(2)	0.2018(2)
0.8	0.1963(3)	0.1264(2)	0.0941(2)	0.4163(4)	0.2768(2)	0.2076(1)
0.9	0.2418(3)	0.1374(1)	0.0970(1)	0.5128(1)	0.3033(3)	0.2152(1)
1.0	0.3002(1)	0.1503(2)	0.1000(1)	0.6664(1)	0.3332(2)	0.2221(1)

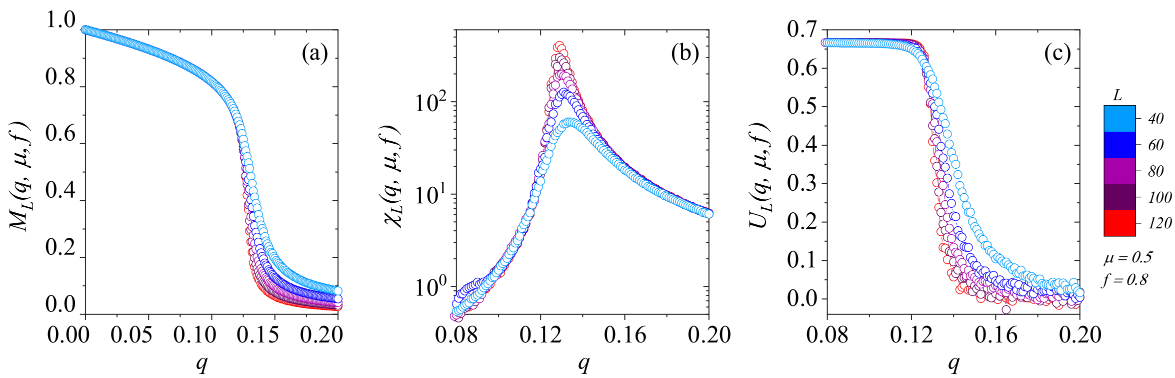

Fig. 7. Size dependence on consensus robustness versus noise parameter. In (a) average opinion, (b) susceptibility and (c) Binder cumulant U for system sizes $L = 40, 60, 80, 100,$ and 120. In this result, $f = 0.8$ and $\mu = 0.5$. The lines are guides to the eyes.

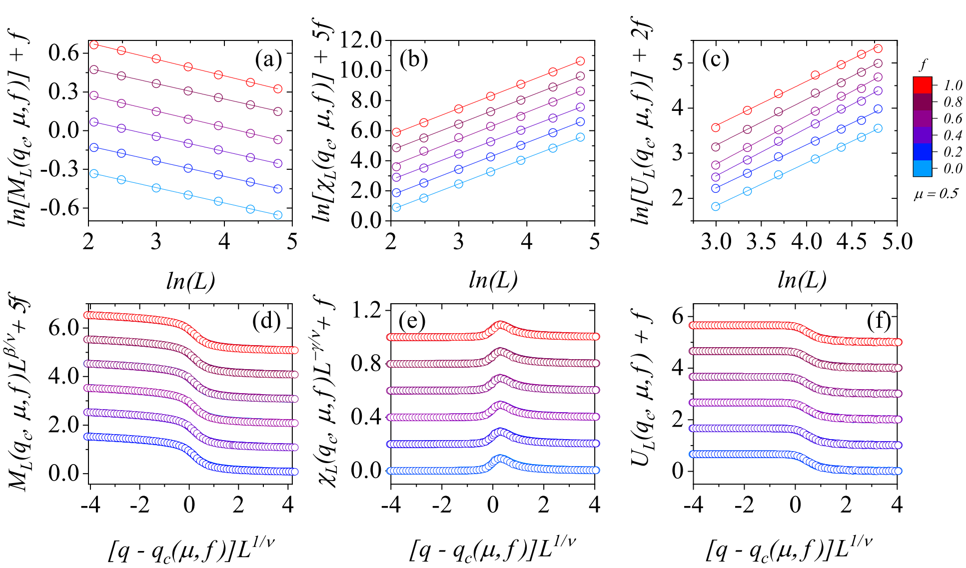

Fig. 8. Finite-size scaling analysis and universality. (a) Magnetization, (b) magnetic susceptibility, and (c) Binder fourth-order cumulant at the critical point $q = q_c(\mu, f)$ as functions of linear system size L in log–log scale for several values of the cooperative fraction f and $\mu = 0.5$. The lines represent linear fits to the data, yielding the standard Ising model critical exponents on square lattices considering error bars. We rescale all quantities, rendering one universal curve for critical exponents $\beta/\nu = 0.125$, $\gamma/\nu = 1.75$, and $1/\nu = 1$. We shift curves up to avoid overlap.

of f. By measuring the linear coefficient of each line in Fig. 8(a), (b) and (c), we estimate $\beta/\nu \approx 0.125$, $\gamma/\nu \approx 1.75$ and $1/\nu \approx 1$ considering the error bars. We confirm our results by performing a data collapse of rescaled versions (d) $\widetilde{M}$, (e) $\widetilde{\chi}$ and (f) $\widetilde{U}$ over the rescaled social noise using $\beta/\nu = 0.125$, $\gamma/\nu = 1.75$ and $1/\nu = 1$. Despite the different behaviors observed in Figs. 3 and 7, Fig. 8(d), (e), and (f) yield a single universal curve independently on f.

We further investigate critical exponents for $\mu = 0.25$ and $\mu = 0.75$, and the results also supply the same set of critical exponents. We conclude that the critical exponents of the cooperative majority-vote model are the same as those in an equilibrium two-dimensional Ising model and for the isotropic majority-vote dynamics [24], regardless of μ and f. This result is under Grinstein's criterion that states that nonequilibrium stochastic spin-like systems with up-down symmetry in

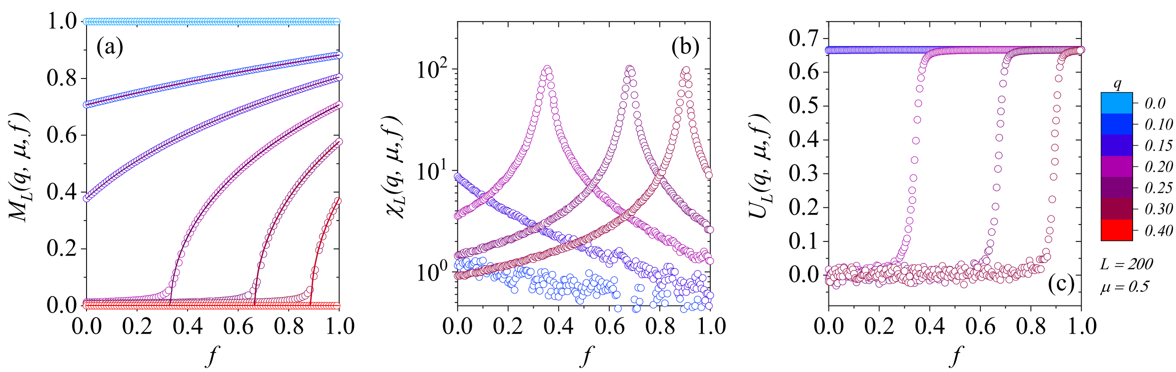

Fig. 9. Plots of the (a) magnetization, (b) magnetic susceptibility, and (c) Binder cumulant as a function of f for several values of the noise q for $\mu = 0.5$. The dashed lines on (a) stand for the analytical results given by Eq. (21), and the symbols are the numerical results for 20 samples with $L = 200$.

regular lattices fall into the same universality class of the equilibrium Ising model [59,60].

3.3. Mean-field analyses

A given configuration of opinions can be denoted by $\sigma = (\sigma_1, \sigma_2, \dots, \sigma_i, \dots, \sigma_N)$, with $N = L^2$. We obtain the behavior of the stationary magnetization m using the master equation that expresses the evolution of the probability $P(\sigma, t)$ of finding the system in the state σ at a time t [61,62]

$$\frac{d}{dt}P(\sigma,t) = \sum_{i=1}^{N}\left[w_i(\sigma^i)P(\sigma^i,t) - w_i(\sigma)P(\sigma,t)\right], \tag{11}$$

where the state σ^i can be obtained from state σ flipping the ith agent's opinion, i.e., $\sigma^i = (\sigma_1, \sigma_2, \dots, -\sigma_i, \dots, \sigma_N)$. Factor w_i is the flip rate of the ith individual $\sigma_i \to -\sigma_i$, given by Eq. (1) for the cooperative voter model. From Eq. (11), it follows that the time evolution of the average opinion of the agent σ_i is

$$\frac{d}{dt}\langle\sigma_i\rangle = -2\langle\sigma_i w_i\rangle. \tag{12}$$

Thus, for all Nf cooperative individuals, we write the following set of equations

$$\frac{d}{dt}\langle\sigma_j\rangle = -\langle\sigma_j\rangle + \Theta_\mu\left\langle S\left(\sum_\delta \sigma_{j+\delta}\right)\right\rangle, \tag{13}$$

for $j = 1, 2, \dots, Nf$, where we replace w_j using Eq. (1) with $\Theta_\mu = 1-2\mu q$ and $\sigma_j^2 = 1$. Similarly, for the remaining $N(1-f)$ agents, we have

$$\frac{d}{dt}\langle\sigma_k\rangle = -\langle\sigma_k\rangle + \Theta\left\langle S\left(\sum_\delta \sigma_{k+\delta}\right)\right\rangle, \tag{14}$$

where $\Theta = 1-2q$ and $k = Nf+1, Nf+2, \dots, N$. Adding Eqs. (13) and (14) and summing for all agents, we obtain

$$\sum_{i=1}^{N}\frac{d}{dt}\langle\sigma_i\rangle = -\sum_{i=1}^{N}\langle\sigma_i\rangle + N\left[f\Theta_\mu + (1-f)\Theta\right]\left\langle S\left(\sum_\delta \sigma_{i+\delta}\right)\right\rangle. \tag{15}$$

In the mean-field limit, a randomly chosen agent σ_i interacts with four neighbors also randomly selected. Labeling these neighbors as σ_a, σ_b, σ_c and σ_d, we write [57,58]

$$S\left(\sum_\delta \sigma_{i+\delta}\right) = S(\sigma_a+\sigma_b+\sigma_c+\sigma_d)$$

$$= \frac{3}{8}(\sigma_a+\sigma_b+\sigma_c+\sigma_d) - \frac{1}{8}(\sigma_a\sigma_b\sigma_c + \sigma_a\sigma_b\sigma_d + \sigma_a\sigma_c\sigma_d + \sigma_b\sigma_c\sigma_d). \tag{16}$$

In addition, in the stationary state, $m \approx \langle\sigma_i\rangle$ and $\langle\sigma_l\sigma_u\sigma_v\rangle \approx \langle\sigma_l\rangle\langle\sigma_u\rangle\langle\sigma_v\rangle \approx m^3$. Thus, we write

$$\left\langle S\left(\sum_\delta \sigma_{i+\delta}\right)\right\rangle = \frac{m}{2}(3-m^2). \tag{17}$$

By using this result in Eq. (15), we obtain

$$\frac{d}{dt}m = m\left\{-\epsilon - \frac{m^2}{2}\left[f\Theta_\mu + (1-f)\Theta\right]\right\}, \tag{18}$$

where

$$\epsilon = 1 - \frac{3}{2}\left[f\Theta_\mu + (1-f)\Theta\right]. \tag{19}$$

In the stationary state, $dm/dt = 0$. For $\epsilon > 0$, there is only one real solution, $m = 0$, representing the paramagnetic state (disordered). For $\epsilon < 0$, we obtain the ferromagnetic state (ordered) solution

$$m = \sqrt{\frac{2|\epsilon|}{f\Theta_\mu + (1-f)\Theta}}, \tag{20}$$

Then, using $\Theta_\mu = 1-2\mu q$ and $\Theta = 1-2q$ and Eq. (19), we write

$$m = \sqrt{\frac{1-6q\left[1-f(1-\mu)\right]}{1-2q\left[1-f(1-\mu)\right]}} \equiv \sqrt{\frac{1-6\bar{q}}{1-2\bar{q}}}, \tag{21}$$

with $\bar{q} = \bar{\mu}q = q[1-f(1-\mu)]$, valid for $q < q_c^{MF}$, the mean-field critical temperature. By imposing $m = 0$ in Eq. (21), we obtain

$$q_c^{MF}(\mu, f) = \frac{1}{6\left[1-f(1-\mu)\right]}. \tag{22}$$

Note that when $f = 0$, Eq. (21) yields the isotropic MVM mean-field result for m

$$m = \sqrt{\frac{1-6q}{1-2q}}, \tag{23}$$

with $q_c^{MF} = 1/6$ [63]. For $f = 1$, $q_c^{MF} = 1/6\mu$ as anticipated. Additionally, near the phase transition, $m \sim (|q - q_c^{MF}|)^\beta$, and we find exponent $\beta = 1/2$, indicating that the cooperative majority-vote model should belong to the mean-field Ising universality class.

3.4. Mean-field simulations

We confirm our mean-field analytical results by performing Monte Carlo simulations in the mean-field approach. In this formulation, we randomly select an agent whose four neighbors are also randomly chosen [38]. We consider systems of $N = L^2$ agents, with L ranging from 40 to 200. We skip 10^3 MCS to allow thermalization and evaluate the time averages over the next 10^5 MCS up to 100 different samples.

In Fig. 9, we show mean-field numerical estimates for (a) $M_L(q,\mu,f)$, (b) $\chi_L(q,\mu,f)$ and (c) $U_L(q,\mu,f)$ as functions of the fraction of collaborative individuals f for several values of the noise q. We evaluate the magnetization numerically (circles) and compare it with the

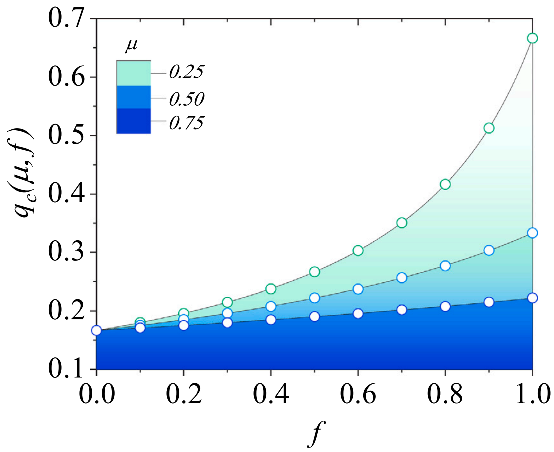

Fig. 10. Mean-field consensus-dissensus phase diagram. Lines denote analytical solutions given by Eq. (22), producing the phase boundaries that separate the ordered and the disordered phases for each noise sensibility μ. Circles represent numerical results for $q_c^{MF}(\mu,f)$, estimated by intersection points of Binder cumulant curves in mean-field simulations.

analytical solution of Eq. (21) (lines), exhibiting a satisfactory agreement. We note that mean-field results match the overall behavior displayed in Fig. 2 for square lattices, in which f improves consensus for different values of social noise q. The small divergence near the phase transition point results from the limited nature of the simulated mean-field network with $N = 4 \times 10^4$, whereas the analytical solution assumes the thermodynamic limit $N \longrightarrow \infty$.

The maximum value of each susceptibility curve in Fig. 9(b) denotes the critical values of f that yield an order–disorder phase transition. Additionally, the critical noise q necessary to vanish the order consensus increases with f, denoting a boost of social robustness. This result combines the behavior observed in Fig. 2(b) and Eq. (22), in which $q_c^{MF}(\mu,f)$ is a monotonically increasing function of f, validating our mean-field analysis.

Fig. 10 shows the mean-field phase diagram in the $q \times f$ parameter space, revealing the boundary between ordered and disordered phases as a function of f and μ. The lines represent the analytical solutions given by Eq. (22), and the circles represent the numerical data estimates obtained from the intersection points of Binder cumulant curves. The mean-field phase diagram shows the same qualitative characteristics of the square lattice scenario of Fig. 6. Numerical results are summarized in Table 1. Finally, we use finite-size scaling relations to plot in Fig. 11(a) magnetization, (b) magnetic susceptibility, and (c) absolute value of the Binder cumulant derivative at the critical temperature $q = q_c^{MF}(\mu,f)$ versus the system size for $\mu = 0.5$. The line slopes estimate critical exponents $\beta \approx 1/2$, $\gamma \approx 1$, and $\nu \approx 2$ for all values of the investigated f and μ. These results confirm the mean-field cooperative majority-vote dynamics belong to the mean-field Ising universality class.

4. Social entropy production

Entropy production is a manifestation of irreversibility dynamics. The cooperative majority-vote model generates entropy, even in the stationary regime; in contrast, reversible models reach thermodynamic equilibrium states without entropy production in the steady state [56–58]. In this context, we consider the Boltzmann–Gibbs entropy equation at time t

$$S(t) = -\sum_{\sigma} P(\sigma,t)\,\ln\,P(\sigma,t). \tag{24}$$

Combining Eq. (24) with the master equation of Eq. (11), we can express the time derivative of entropy as

$$\frac{d}{dt}S(t) = \frac{1}{2}\sum_{\sigma}\sum_{i}\left[w_i(\sigma^i)P(\sigma^i,t) - w_i(\sigma)P(\sigma,t)\right]\ \ln\,\frac{P(\sigma^i,t)}{P(\sigma,t)}, \tag{25}$$

We frame the rate of change of the entropy S of a system as two main components: entropy production rate Π and entropy flux Φ from system to environment. Thus, we write

$$\frac{d}{dt}S(t) = \Pi - \Phi. \tag{26}$$

Therefore, comparing Eqs. (25) and (26)

$$\Pi = \frac{1}{2}\sum_{\sigma}\sum_{i}\left[w_i(\sigma^i)P(\sigma^i,t) - w_i(\sigma)P(\sigma,t)\right]\ \ln\,\frac{w_i(\sigma^i)P(\sigma^i,t)}{w_i(\sigma)P(\sigma,t)}, \tag{27}$$

and

$$\Phi = \frac{1}{2}\sum_{\sigma}\sum_{i}\left[w_i(\sigma^i)P(\sigma^i,t) - w_i(\sigma)P(\sigma,t)\right]\ \ln\,\frac{w_i(\sigma^i)}{w_i(\sigma)}, \tag{28}$$

Note that Π is positive definite, but Φ can assume either sign depending on the direction of the flux. We write

$$\Phi = \sum_{\sigma}\sum_{i} w_i(\sigma)P(\sigma,t)\ \ln\,\frac{w_i(\sigma)}{w_i(\sigma^i)}, \tag{29}$$

that allows numerical estimates [64–69].

4.1. Flux on square lattices

The flux of entropy as a configurational average over the probability distribution in the stationary state from Eq. (29) is

$$\Phi = \sum_{i}\left\langle w_i(\sigma)\ \ln\,\frac{w_i(\sigma)}{w_i(\sigma^i)}\right\rangle. \tag{30}$$

The social entropy S remains constant in this state, therefore $\Pi = \Phi$. Hence, we calculate the stationary social entropy production by employing Monte Carlo simulations using Eq. (30).

In Fig. 12, we plot numerical results of entropy production $\varphi_L(q,\mu,f)$ in the stationary regime for several values of (a) system size L, (b) collaborative fraction f and (c) noise attenuation μ versus q. We observe in (a) that entropy flux has a weak sensibility with population size but a strong dependence on the fraction of collaborative agents and noise attenuation. Curves for $f = 0.0$ and $\mu = 1.0$ in Fig. 12(b) and (c), respectively, display the flux of entropy of the isotropic MVM [24,25], where a maximum flux occurs after the critical noise $q_c(\mu, f = 0.0) = 0.075$ and tends to zero for $q \to 0$ or $q \to 1/2$ in the isotropic case.

We highlight Fig. 12(b) also displays entropy flux that follows the isotropic system under the linear transformation $q \to q/\mu$, when $f = 1.00$ and $\mu = 0.5$. This flux vanishes for $q \to 0$ and $q \to 1/2\mu$. For $0 < f < 1$, after the maximum, instead of approaching zero, the entropy flux increases, supported by a discrepancy between the behavior of the cooperative and regular individuals. Indeed, (c) reveals this phenomenon intensifies as μ becomes smaller since the social temperature disparity among agents increases. We remark that, in general, a combination of cooperative and non-cooperative individuals increases the social entropy production of the society. Nonetheless, for small values of the social noise, the entropy generation is maximized when there is no cooperative behavior, $f = 0.0$.

For non-equilibrium systems, such as the cooperative majority-vote model, the Maximum Entropy Production Principle proposes that among all possible non-equilibrium steady states (NESS) that satisfy the system's constraints, the one with the highest entropy production rate is the most likely. The NESS with higher entropy production does not necessarily have more disorder but yields a dynamic balance that maximizes entropy production. Hence, if real-world societies follow this principle, the heterogeneity between cooperative and non-cooperative individuals could be a potential natural manifestation of the achieved NESS [70,71].

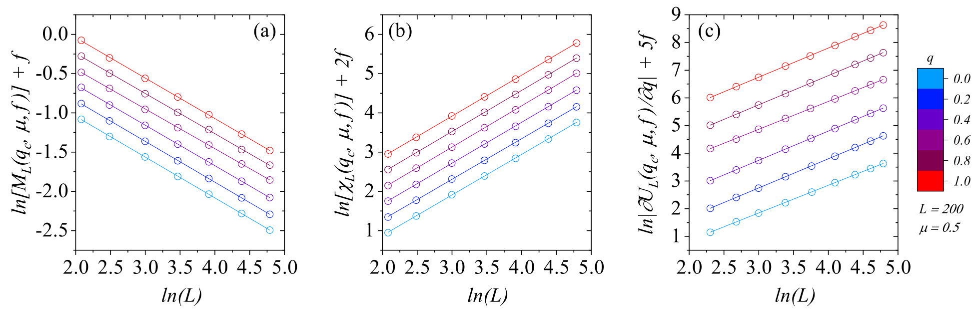

Fig. 11. Mean-field finite-size estimates for critical exponents. (a) $M(q,\mu,f)$, (b) $\chi(q,\mu,f)$ and (c) $|\partial U(q,\mu,f)/\partial q|$ with $q = q_c^{MF}(\mu,f)$ versus system size L for $\mu = 0.5$. Lines are linear regressions to the data, and their slopes equal the respective critical exponents in the mean-field limit.

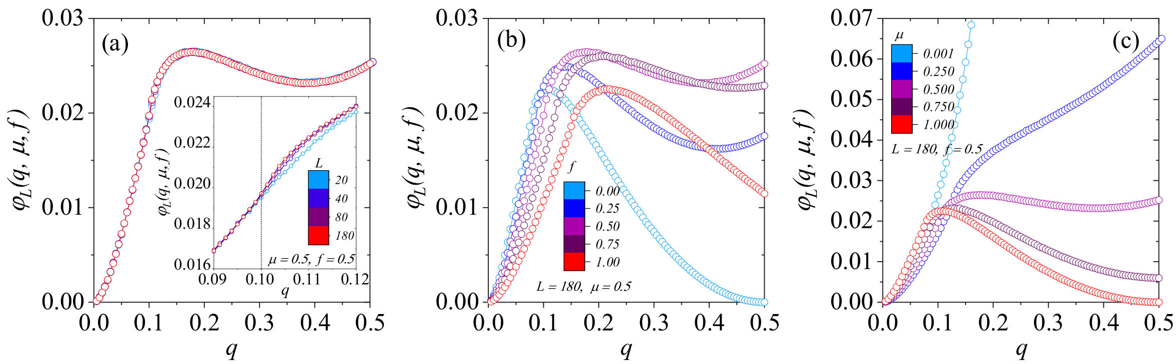

Fig. 12. Stationary social entropy flux production for collaborative majority-vote opinion dynamics versus noise parameter. We plot $\varphi_L(q,\mu,f)$ vs. q for several values of (a) system size L, (b) cooperative fraction f and (c) noise attenuation μ on square lattices. On (a) $\mu = 0.5$ and $f = 0.5$, while in (b) $\mu = 0.5$ and (c) $f = 0.5$ with $L = 180$. The lines are guides to the eyes.

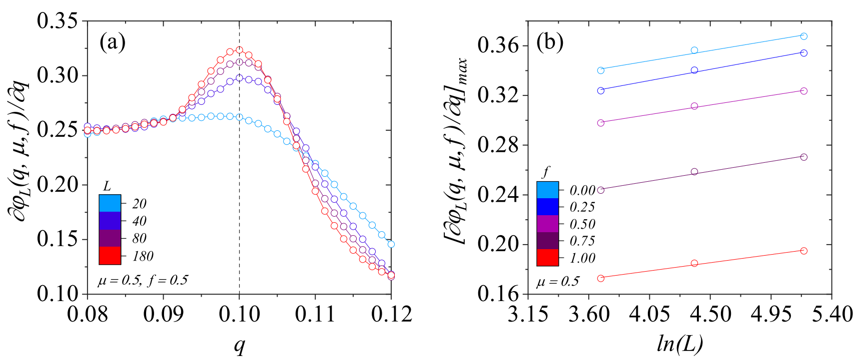

Fig. 13. Entropy flux Size dependence. (a) Derivative of entropy flux versus q for $\mu = 0.5$ and $f = 0.5$. (b) Maximum value of the entropy flux derivative at the critical point as a function of the natural logarithmic of the system size L. From top to bottom, line slopes are $\eta = 0.018(3), 0.020(2), 0.017(1), 0.018(2)$ and $0.015(2)$.

As a general pattern, the critical temperature does not coincide with the maximum of $\varphi_L(q,\mu,f)$. In fact, the critical noise is the point of inflection for φ that occurs before the maximum point. We display this behavior in the inset of Fig. 12(a), in which for $\mu = 0.5$ and $f = 0.5$, we obtain $q_c = 0.1011(1)$ (see Table 1). Therefore, in analogy with the entropy of equilibrium Ising model, the entropy flux exhibits a finite singularity at the critical point as

$$\varphi_L(q,\mu,f) = \varphi_L[q_c,\mu,f] + A_\pm \left|q - q_c\right|^{(1-\alpha)}, \tag{31}$$

where $A_\pm$ are amplitudes of regimes above and under the critical point $q_c = q_c(\mu,f)$ [57,58]. Hence, instead of a maximum in entropy flux, the second-order phase transition maximizes the derivative of entropy flux with respect to q, as we can observe in Fig. 13(a) for $q_c(0.5,0.5) = 0.1011(1)$. Indeed, from Eq. (31), we obtain

$$\frac{\partial\varphi_L(q,\mu,f)}{\partial q} \sim \left|q - q_c\right|^{-\alpha}, \tag{32}$$

where α corresponds to the same exponent associated with the specific heat of the Ising model. On square lattices, $\alpha = 0$, generating a singularity of the logarithm type. Hence, in analogy to the Ising model, we write

$$\frac{\partial\varphi_L(q,\mu,f)}{\partial q} \sim \ln\left|q - q_c\right|. \tag{33}$$

To verify our conjecture, we use the Savitzky-Golay Smooth algorithm with cubic polynomials to numerically estimate $\partial\varphi_L(q,\mu,f)/\partial q$ for several sizes L in Fig. 13(a). By finite-size scaling theory on Eq. (33), the maximum value of the partial derivative of entropy flux must diverge at the critical point as

$$\left[\frac{\partial\varphi_L(q,\mu,f)}{\partial q}\right]_{max} \sim \ln\, L^{\eta}, \tag{34}$$

with $\eta = (1-\zeta)/\nu$ and ν is the critical exponent associated to correlation length. Indeed, our results support $\nu = 1.0$, leading to $\zeta \approx 1.0$. Fig. 13(b) confirms our assumption for $\mu = 0.5$ and several cooperative fraction values. We observe the same behavior for other values of μ and f.

4.2. Mean-field approach

The mean-field theory allows us to develop an analytical expression for entropy flux in the stationary regime. From Eq. (1), we write

$$\ln\frac{w_i(\sigma)}{w_i(\sigma^i)} = \ln\left[\frac{1-\sigma_i S\left(\sum_\delta \sigma_{i+\delta}\right) + 2\mu_i q\sigma_i S\left(\sum_\delta \sigma_{i+\delta}\right)}{1+\sigma_i S\left(\sum_\delta \sigma_{i+\delta}\right) - 2\mu_i q\sigma_i S\left(\sum_\delta \sigma_{i+\delta}\right)}\right].$$

Next, we note that the product $\sigma_i S\left(\sum_\delta \sigma_{i+\delta}\right)$ may assume only one of three possible values: $-1, 0$ and 1. Therefore,

$$\ln\frac{w_i(\sigma)}{w_i(\sigma^i)} = \begin{cases} \ln\left(\frac{\mu_i q}{1-\mu_i q}\right)\times(1), & \text{if } \sigma_i S\left(\sum_\delta \sigma_{i+\delta}\right) = 1, \\ \ln\left(\frac{\mu_i q}{1-\mu_i q}\right)\times(0), & \text{if } \sigma_i S\left(\sum_\delta \sigma_{i+\delta}\right) = 0, \\ \ln\left(\frac{\mu_i q}{1-\mu_i q}\right)\times(-1), & \text{if } \sigma_i S\left(\sum_\delta \sigma_{i+\delta}\right) = -1. \end{cases}$$

Thus, we obtain

$$\ln\frac{w_i(\sigma)}{w_i(\sigma^i)} = \ln\left[\frac{\mu_i q}{1-\mu_i q}\right]\sigma_i S\left(\sum_\delta \sigma_{i+\delta}\right). \tag{35}$$

Combining Eqs. (30) and (35)

$$\Phi = \sum_{j=1}^{Nf}\left\langle \ln\left[\frac{\mu q}{1-\mu q}\right]\sigma_j S\left(\sum_\delta \sigma_{j+\delta}\right) w_j(\sigma)\right\rangle$$

$$+ \sum_{k=Nf+1}^{N}\left\langle \ln\left[\frac{q}{1-q}\right]\sigma_k S\left(\sum_\delta \sigma_{k+\delta}\right) w_k(\sigma)\right\rangle. \tag{36}$$

Furthermore, in the stationary state, we obtain

$$\left\langle \left[S\left(\sum_\delta \sigma_{j+\delta}\right)\right]^2\right\rangle = \frac{1}{8}\left(5+6m^2-3m^4\right). \tag{37}$$

We divide Eq. (36) by the total number of individuals N and combine it with Eqs. (1) and (37) to derive an expression for entropy flux per site:

$$\begin{gathered}\varphi \equiv \Phi/N = f\,\ln\left(\frac{\mu q}{1-\mu q}\right)\times \\ \left[\frac{1}{4}(3m^2-m^4) - \frac{\Theta_\mu}{16}(5+6m^2-3m^4)\right] \\ +(1-f)\,\ln\left(\frac{q}{1-q}\right)\times \\ \left[\frac{1}{4}(3m^2-m^4) - \frac{\Theta}{16}(5+6m^2-3m^4)\right].\end{gathered} \tag{38}$$

We set $m = 0$ and get the disordered solution of the entropy flux, valid for $q > q_c^{MF}(\mu, f)$:

$$\varphi = \frac{5}{16}f\Theta_\mu\,\ln\left(\frac{1-\mu q}{\mu q}\right) + \frac{5}{16}(1-f)\Theta\,\ln\left(\frac{1-q}{q}\right). \tag{39}$$

On the ordered state, we have that magnetization behaves accordingly to Eq. (21), which is valid for $q < q_c^{MF}(\mu, f)$. Combining Eqs. (21) and (38), we obtain the entropy flux expression in the ferromagnetic state:

$$\varphi = \frac{f}{(1-2\bar{q})^2}\,\ln\left(\frac{1-\mu q}{\mu q}\right)\left\{\bar{q}\left[3-\Theta_\mu(2+\bar{q})\right]-\mu q\right\}$$

$$+\frac{1-f}{(1-2\bar{q})^2}\,\ln\left(\frac{1-q}{q}\right)\left\{\bar{q}\left[3-\Theta(2+\bar{q})\right]-q\right\}, \tag{40}$$

with $\bar{q} = \bar{\mu}q = q[1-f(1-\mu)]$. For the particular case $f = 0.0$, we combine Eqs. (39) and (40) to obtain an expression for entropy production of the isotropic majority-vote model:

$$\varphi(q) = \left(\frac{q}{1-2q}\right)^2(3+2q)\,\ln\left(\frac{1-q}{q}\right)H(q_c - q)$$

$$+\frac{5}{16}(1-2q)\,\ln\left(\frac{1-q}{q}\right)H(q-q_c), \tag{41}$$

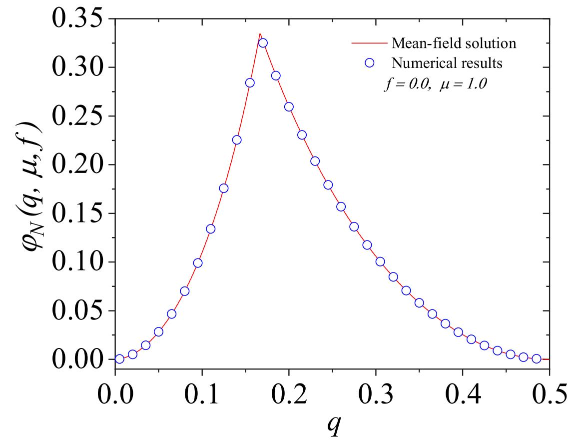

Fig. 14. Entropy production for mean-field isotropic majority-vote model. The red line denotes the results from Eq. (41) and blue circles are numerical estimations and $N = 180 \times 180 = 32400$.

where $H(t)$ is the Heaviside function and $q_c^{MF}(\mu, f = 0.0) = 1/16$ is the isotropic mean-field MVM critical noise. We further investigate numerical simulations in the mean-field formulation to demonstrate this result.

Fig. 14 reveals mean-field entropy flux $\varphi(q, \mu, f)$ versus q, with $N = 180 \times 180 = 32400$, for the isotropic mean-field MVM simulation ($f = 0$ and $\mu = 1.0$). The red line represents results from Eq. (41), where blue circles represent numerical data in the mean-field formulation. Note that φ exhibits a singularity in mean-field critical noise $q_c^{MF} = 1/6$ and vanishes for $q \to 0$ and $q \to 1/2$.

We extend our investigation for mean-field stationary social entropy flux production $\varphi(q, \mu, f)$ versus noise q for several values of the cooperative fraction f and noise sensibility μ. In Fig. 15(a), we set $\mu = 0.5$ and $f = 0.00, 0.25, 0.50, 0.75$ and 1.00, while in Fig. 15(b), $f = 0.5$ and μ assume 0.25, 0.50, 0.75 and 1.00. The open circles are mean-field numerical data for $N = 32400$ individuals, and the lines represent the analytical results given by Eqs. (39) and (40). There are slight deviations between mean-field solutions and Monte Carlo data in the ferromagnetic phase for entropy flux due to the finite nature of simulated systems, amplified as $\mu \to 0$.

Fig. 15(c) shows that φ does not approach zero when $q = 0.5$ in the mean-field limit for $0 < f < 1$ but remains finite independently of system size N. However, for any isotropic case ($f = 0$ or $\mu = 1.0$), φ tends to zero for $q = 0.5$, as expected. Distinguished from the square lattice case, in which φ reaches a maximum for $q > q_c$, in the mean-field framework, the maximum entropy flux point occurs at the mean-field critical temperature q_c^{MF}.

5. Final remarks

This work explores the impacts of collaborative behavior on majority-vote opinion dynamics and its social entropy production. We randomly select a fraction f of individuals of the society to represent cooperative agents, while the complementary fraction $1-f$ are regular voters. We introduce a social noise q such that with probability $(1-q)$, individuals agree with each other regarding a social issue subject, such as a political, professional, or economic matter. The cooperative agents retain a social temperature sensibility $0 < \mu < 1$, experiencing an effective social noise of μq, favoring social validation-based decisions. For $\mu = 0$ and $\mu = 1$, we recover bimodal [36,41] and isotropic majority-vote model [24,25], respectively.

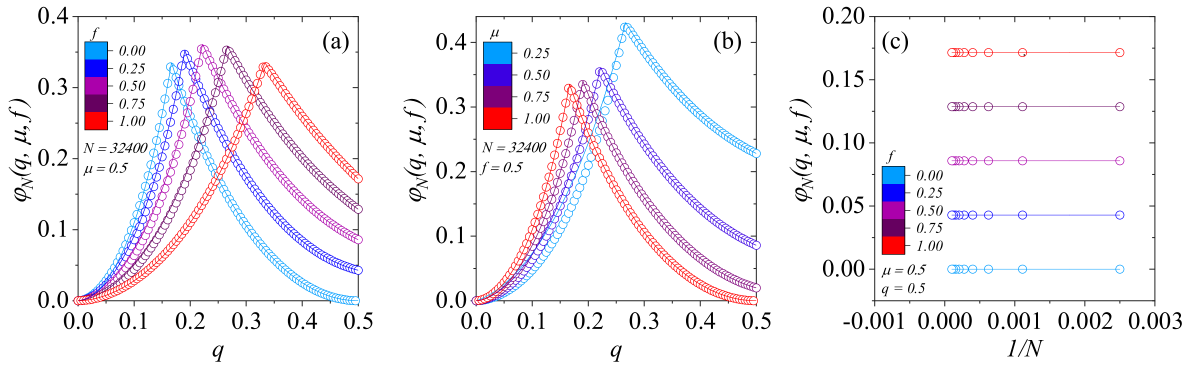

Fig. 15. Mean-field stationary social entropy flux production as a function of the social temperature. (a) Flux production dependence on cooperative fraction f for $\mu = 0.5$, (b) and several values of noise sensibility μ with $f = 0.5$. Open circles are numerical data from mean-field Monte Carlo simulations with $N = 32400$, and lines represent analytical results of Eqs. (39) and (40). Fig. (c) illustrates the finite behavior of entropy flux production for $q = 0.5$ which is independent of system size.

We employ Monte Carlo simulations and find that the system undergoes a second-order consensus-dissensus phase transition with the same universality class of 2D equilibrium Ising model for critical noise values $q = q_c(\mu, f)$. The critical exponents are not affected by the presence of collaborative agents, following Grinstein's criterion which states that nonequilibrium stochastic spin-like systems with up-down symmetry in regular lattices fall into the same universality class of the equilibrium Ising model [59,60].

For heterogeneous societies ($0 < f < 1$), there is a contrast between the effects of social temperature among regular and cooperative individuals, and $q_c(\mu, f)$ is a monotonically decreasing (increasing) function of noise attenuation μ (cooperative fraction f). Indeed, increasing the cooperative fraction f promotes the formation of a giant cluster of agreeing individuals that suppresses the phase transition. The collaborative behavior phenomena enhance the social robustness of society to opinion polarization. We highlight that if all individuals are cooperative ($f = 1.0$), the system behaves as if all individuals were regular ($f = 0.0$) under the linear transformation $q \longrightarrow q/\mu$.

Gibbs entropy and the master equation yield an expression that enables us to compute social entropy production in the stationary regime for square lattices. We observe that the entropy production of the isotropic majority-vote model has a maximum that occurs after the critical noise $q_c(\mu, f = 0.0) = 0.075$ and vanishes for $q \to 0$ or $q \to 1/2$. However, for cooperative societies, the entropy production increases after the local maximum and is non-zero for $q = 1/2$ due to the social temperature disparity between the collaborative and regular agents. Furthermore, combining cooperative and non-cooperative individuals yields higher social entropy production. Yet, for small social noise values, maximum entropy generation occurs in the absence of cooperative behavior, with $f = 0.0$.

Further generalizations of heterogeneous majority-vote opinion dynamics may consider complex network framework and the presence of non-compliance agents, in other words, $\mu > 1$. Exploring the influence of these dissenting agents within opinion dynamics can provide a deeper understanding of societal and (non)cooperative behaviors.

CRediT authorship contribution statement

Igor V.G. Oliveira: Writing – review & editing, Writing – original draft, Software, Methodology, Investigation, Formal analysis, Conceptualization. **Chao Wang:** Writing – review & editing, Writing – original draft, Validation, Investigation, Funding acquisition, Formal analysis, Conceptualization. **Gaogao Dong:** Writing – review & editing, Validation, Formal analysis. **Ruijin Du:** Writing – review & editing, Validation. **Carlos E. Fiore:** Writing – review & editing, Writing – original draft, Validation, Methodology, Investigation, Formal analysis, Data curation, Conceptualization. **André L.M. Vilela:** Writing – review & editing, Writing – original draft, Validation, Supervision, Software, Project administration, Methodology, Investigation, Funding acquisition, Formal analysis. **H. Eugene Stanley:** Supervision, Funding acquisition.

Declaration of competing interest

The authors declare that they have no known competing financial interests or personal relationships that could have appeared to influence the work reported in this paper.

Data availability

Data will be made available on request.

Acknowledgments

We thank M. J. de Oliveira for a critical reading of the manuscript. The authors acknowledge financial support from Brazilian and Chinese institutions and funding agents UPE, FACEPE (APQ-0565-1.05/14, APQ-0707-1.05/14), CAPES, CNPq (306068/2021-4), National Natural Science Foundation of China (72071006, 61603011, 62373169), and National Statistical Science Research Project (2022LZ03). The Boston University Center for Polymer Studies is supported by National Science Foundation, United States Grants PHY-1505000, CMMI-1125290, and CHE-1213217, by DTRA, United States Grant HDTRA1-14-1-0017, and by DOE, United States Contract DE-AC07-05Id14517.

References

[1] Ball P. The physical modelling of society: a historical perspective. Physica A 2002;314(1–4).
[2] Feng L, Li B, Preis T, Stanley HE. Linking agent-based models and stochastic models of financial markets. Proc Natl Acad Sci USA 2012;109(22).
[3] Hilbe C, Wu B, Traulsen A, Nowak MA. Cooperation and control in multiplayer social dilemmas. Proc Natl Acad Sci USA 2014;18(46).
[4] Schweitzer F. Sociophysics. Phys Today 2018;71(2).
[5] Galam S. Sociophysics: A review of galam models. Internat J Modern Phys C 2008;19(3).
[6] Galam S, Moscovici S. Towards a theory of collective phenomena: Consensus and attitude changes in groups. Eur J Soc Psychol 1991;21(1).
[7] Yeomans JM. Statistical mechanics of phase transitions. Clarendon Press; 1992.
[8] Galam S. Rational group decision making: A random field ising model at T=0. Physica A 1997;238(1–4).
[9] Tomé T, de Oliveira MJ. Role of noise in population dynamics cycles. Phys Rev E 2009;79(6).
[10] Schawe H, Hernández L. Higher order interactions destroy phase transitions in deffuant opinion dynamics model. Commun Phys 2022;5(32).
[11] Iacopini I, Petri G, Barrat A, Latorra V. Simplicial models of social contagion. Nature Commun 2019;10(2485).
[12] Centola D. The spread of behavior in an online social network experiment. Science 2010;329(5996).
[13] Stauffer D, de Oliveira SMM, de Oliveira PMC, de Sá Martins JS. Biology, sociology, geology by computational physicists. Elsevier; 2006.

[14] Lu Xi, Mo Hongming, Deng Yong. An evidential opinion dynamics model based on heterogeneous social influential power. Chaos Solitons Fractals 2015;73.
[15] Galam S. Application of statistical physics to politics. Physica A 1999;274(1–2).
[16] Sznajd-Weron K, Sznajd J. Opinion evolution in closed community. Internat J Modern Phys C 2000;11(06).
[17] Kononovicius Aleksejus. Supportive interactions in the noisy voter model. Chaos Solitons Fractals 2021;143.
[18] Nyczka P, Sznajd-Weron K. Anticonformity or independence?—insights from statistical physics. J Stat Phys 2013;151(1–2).
[19] Sznajd-Weron K, Szwabiński J, Weron R. Is the person-situation debate important for agent-based modeling and vice-versa? PLoS One 2014;9(11).
[20] Stone TE, McKay SR. Critical behavior of disease spread on dynamic small-world networks. Europhys Lett 2011;95(3).
[21] Sznajd-Weron K, Sznajd J. Who is left, who is right? Physica A 2005;351(2–4).
[22] Sznajd-Weron K, Weron R. How effective is advertising in duopoly markets? Physica A 2003;324(1–2).
[23] Galam S, Zucker J. From individual choice to group decision-making. Physica A 2000;287(3–4).
[24] de Oliveira MJ. Isotropic majority-vote model on a square lattice. J Stat Phys 1992;66(1).
[25] de Oliveira MJ, Mendes JFF, Santos MA. Nonequilibrium spin models with ising universal behaviour. J Phys A: Math Gen 1993;26.
[26] Chen H, Shen C, He G, Zhang H, Hou Z. Critical noise of majority-vote model on complex networks. Phys Rev E 2015;91(2).
[27] Chen H, Wang S, Shen C, Zhang H, Bianconi G. Non-markovian majority-vote model. Phys Rev E 2020;102(6).
[28] Lima JRS, Lima FWS, Alves TFA, Alves GA, Macedo-Filho A. Diffusive majority-vote model. Phys Rev E 2022;105(3).
[29] Campos Paulo RA, de Oliveira Viviane M, Brady Moreira FG. Small-world effects in the majority-vote model. Phys Rev E 2003;67(2).
[30] Choi J, Goh K. Majority-vote dynamics on multiplex networks with two layers. New J Phys 2019;21(3).
[31] Krawiecki A, Gradowski T, Siudem G. Majority-vote model on multiplex networks. Acta Phys Polon A 2018;133(6).
[32] Pereira Luiz FC, Brady Moreira FG. Majority-vote model on random graphs. Phys Rev E 2005;71(1).
[33] Lima FWS. Majority-vote on undirected barabási-albert networks. Commun Comput Phys 2007;2(2).
[34] Crokidakis N, de Oliveira PMC. Impact of site dilution and agent diffusion on the critical behavior of the majority-vote model. Phys Rev E 2012;85(4).
[35] Vilela André LM, Brady Moreira FG. Majority-vote model with different agents. Physica A 2009;388(19).
[36] Vilela André LM, Brady Moreira FG, de Souza Adauto JF. Majority-vote model with a bimodal distribution of noises. Physica A 2012;391(24).
[37] Lima FWS. Majority-vote model with heterogeneous agents on square lattice. Internat J Modern Phys C 2013;24(11).
[38] Vieira AR, Crokidakis N. Phase transitions in the majority-vote model with two types of noises. Physica A 2016;450.
[39] Encinas JM, Chen Hanshuang, de Oliveira Marcelo M, Fiore Carlos E. Majority-vote model with ancillary noise in complex networks. Physica A 2019;(516).
[40] Wu ZX, Holme P. Majority-vote model on hyperbolic lattices. Phys Rev E 2010;81(1).
[41] Vilela André LM, de Souza Adauto JF. Majority-vote model with a bimodal distribution of noises in small-world networks. Physica A 2017;488.
[42] Vilela André LM, Pereira Luiz FC, Dias L, Stanley HE, da Silva Luciano R. Majority-vote model with limited visibility: An investigation into filter bubbles. Physica A 2021;563.
[43] Vilela André LM, Stanley HE. Effect of strong opinions on the dynamics of the majority-vote model. Sci Rep 2018;8(1).
[44] Santos MA, Teixeira S. Anisotropic voter model. J. Stat. Phys. 1995;78(3–4).
[45] Costa LSA, de Souza AJF. Continuous majority-vote model. Phys Rev E 2005;71(5).
[46] Melo Diogo FF, Pereira Luiz FC, Brady Moreira FG. The phase diagram and critical behavior of the three-state majority-vote model. J Stat Mech Theory Exp 2010;2010(11).
[47] Lima FWS. Three-state majority-vote model on square lattice. Physica A 2012;391(4).
[48] Vilela André LM, Zubillaga Bernardo J, Wang Chao, Wang M, Du Ruijin, Stanley HE. Three-state majority-vote model on scale-free networks and the unitary relation for critical exponents. Sci Rep 2020;10.
[49] Vilela André LM, Wang Chao, Nelson Kenric P, Stanley HE. Majority-vote model for financial markets. Physica A 2019;515.
[50] Zubillaga Bernardo J, Vilela André LM, Wang Chao, Nelson Kenric P, Stanley HE. A three-state opinion formation model for financial markets. Physica A 2022;588.
[51] Granha Mateus FB, Vilela André LM, Wang Chao, Nelson Kenric P, Stanley HE. Opinion dynamics in financial markets via random networks. Proc Natl Acad Sci 2022;119(49).
[52] Zha Q, Kou G, Zhang H, Liang H, Chen X, Li C, Dong Y. Opinion dynamics in finance and business: a literature review and research opportunities. Financ Innov 2020;6(1).
[53] Capraro V. A model of human cooperation in social dilemmas. PLoS One 2013;8(8).
[54] de Jong G, Veijer J. Cooperative behavior in strategic decision making: Human capital and personality traits. Behav Strateg: Emerg Perspect 2014.
[55] Pennisi E. How did cooperative behavior evolve? Science 2005;309(5731).
[56] Tomé T, de Oliveira MJ. Entropy production in nonequilibrium systems at stationary states. Phys Rev Lett 2012;108(2).
[57] Hawthorne Felipe, Harunari Pedro E, de Oliveira MJ, Fiore Carlos E. Nonequilibrium thermodynamics of the majority-vote model. Phys Rev E 2023;(25).
[58] Fernández Noa CE, Harunari Pedro E, de Oliveira MJ, Fiore CE. Entropy production as a tool for characterizing nonequilibrium phase transitions. Phys Rev E 2019;(100).
[59] Grinstein G, Jayaprakash C, He Y. Statistical mechanics of probabilistic cellular automata. Phys Rev Lett 1985;55(23).
[60] Baxter RJ. The inversion relation method for some two-dimensional exactly solved models in lattice statistics. J Stat Phys 1982;28(1).
[61] Van Kampen NG. Stochastic processes in physics and chemistry. Elsevier; 2007.
[62] Tomé Tânia, Fiore Carlos E, de Oliveira Mário J. Stochastic thermodynamics of opinion dynamics models. Phys Rev E 2023;(107).
[63] Tomé T, de Oliveira MJ. Stochastic dynamics and irreversibility. Springer; 2015.
[64] Nicolis G, Prigogine Ilya. Self-organization in nonequilibrium systems: from dissipative structures to order through fluctuations. Wiley; 1977.
[65] Lebowitz JL, Spohn H. A gallavotti-cohen-type symmetry in the large deviation functional for stochastic dynamics. J Stat Phys 1999;95(1–2).
[66] Maes C. The fluctuation theorem as a gibbs property. J Stat Phys 1999;95(1).
[67] Maes C, Redig F, Moffaert AV. On the definition of entropy production, via examples. J Math Phys 2000;41(3).
[68] Maes C, Netočnỳ K. Time-reversal and entropy. J Stat Phys 2003;110(1).
[69] Lecomte V, Rácz Z, Van Wijland F. Energy flux distribution in a two-temperature ising model. J Stat Mech Theory Exp 2005;2005(2).
[70] Martyushev LM, Seleznev VD. Maximum entropy production principle in physics, chemistry and biology. Phys Rep 2006;426(1).
[71] Dyke J, Kleidon A. The maximum entropy production principle: Its theoretical foundations and applications to the earth system. Entropy 2010;12(3).